Crossref
DOI: 10.31643/2026/6445.32
Earth Sciences

Acoustoemission of Graphite and Graphene

[1*]Zhangozin K.N., [2]Yurov V.M., [3]Kargin D.B.

[1]LLP Vostok, Astana, Kazakhstan
[2]LLP Vostok, Karaganda, Kazakhstan
[3]NAO L.N. Gumilyov Eurasian National University, Astana, Kazakhstan

**Corresponding author email 4kzh@mail.ru*

Received: *February 26, 2025*
Peer-reviewed: *April 15, 2025*
Accepted: *May 2, 2025*

ABSTRACT
In this paper, we propose a model of the acoustic emission mechanism of natural graphite and graphene. The thickness of the surface layer R(I) of graphite varies from 0.9 nm in the parallel to 2.46 nm in the perpendicular plane and contains three graphene monolayers. Corrugations on the surface of free graphene arise due to high internal stresses, leading to significant deformation energy. An estimate of the deformation energy associated with the reconstruction of the surface of graphite and graphene is proposed. We imagine a graphite nanolayer as a potential well with infinitely high walls, then the energy levels of the nanolayer are determined by one fundamental parameter - the lattice constant of the crystal. The lattice constant a changes in the R(I) layer due to size effects. As soon as the parameter a stops changing, the spectrum of quantum states passes into a continuous spectrum, where the classical Drude–Lorentz laws are fulfilled for graphite. Since the surface layer of graphite is a two-dimensional quantum medium, three quantum planes of graphite with a_1, a_2 and a_3 should be considered. The article considers one-, two- and three-layer graphene. The Fermi surface of graphene degenerates into the Dirac point, and the Fermi energy is zero. For two-layer graphene, the Fermi energy is E_F = 0.9 eV, and for three-layer graphene - E_F = 1.2 eV. Namely, all three quantum levels participate in the acoustic emission of graphite and graphene. In the article, it can be considered proven that in natural graphite (as well as in all solids), acoustic emission occurs due to the reconstruction of its surface, leading to the emergence of a surface layer R(I) and deformation energy E_d. The article proposes a thermoacoustics model that contains only experimentally determined parameters, and their accuracy is quite acceptable.

Keywords: acoustic emission, graphite, graphene, nanolayer, Fermi surface, crystal.

Information about authors:

Zhangozin Kanat Nakoshevich — *Director, Leading Researcher of TSK-Vostok LLP, Candidate of Physical and Mathematical Sciences, Associate Professor, Saryarka District, Republic Avenue, Building 3/2, Apartment 40, Astana, Kazakhstan. E-mail: 4kzh@mail.ru; ORCID ID: https://orcid.org/0000-0003-1234-0486*

Yurov Viktor Mikhailovich — *Leading researcher of TSK-Vostok LLP, candidate of physical and mathematical sciences, associate professor, Gogol street, house 51, apartment 55, Karaganda, Kazakhstan. E-mail: exciton@list.ru; ORCID ID: https://orcid.org/0000-0002-7918-9656*

Kargin Djumat Beisenbekovich — *Candidate of Physical and Mathematical Sciences, Associate Professor, Director of the Department of Technology Commercialization, L.N. Gumilyov Eurasian National University, Satpayev street building 2, Astana, Kazakhstan. E-mail: kargin_db@enu.kz; ORCID ID: https://orcid.org/0000-0002-1027-6428*

Introduction

Until the mid-20th century, graphite was used as pencils, electrodes, anodes, etc. Then it began to be used in metal production, in atomic and nuclear power engineering, in aviation and space technology [[1], [2], [3]]. The end of the 20th and the beginning of the 21st century were marked by the discovery of fullerenes (1985) [4], carbon nanotubes (1991) [5] and graphenes (2004) [6]. Carbon nanowalls, carbon sheets, nanocrystalline graphite, etc., have acquired a special role at present [7].

In Kazakhstan, Ushtogan LLP plans to mine graphite ores using an open pit method from the Sarytoganbai deposit in the Aktogai district of the Karaganda region. The subsoil user has already submitted a plan for developing the deposit for 2025-2049 on the Unified Ecological Portal of Kazakhstan. Studies have shown that the content of graphite from this deposit in the concentrate can be increased to 99.998%, and, importantly, without acid cleaning. The hydrometallurgical method is most suitable for enrichment.

We have developed a method for obtaining graphene from the graphite of this deposit by intercalating graphite with microcluster water. Further, the graphene additive is used to obtain concrete, which is very much needed for industrial enterprises in Kazakhstan. To obtain high-quality graphene concrete, it is necessary to use non-destructive testing [8], among which the acoustic emission method is of particular importance. However, to apply this method, it is necessary to know the structure of the graphite surface layer and the production of graphene from it, as well as their acoustic properties. The speed of acoustic waves in graphite is still being studied [9], but the mechanism of their occurrence, in addition to thermal vibrations, remains unknown to date.

The aim of this work is to clarify the mechanism of acoustic emission of natural graphite and graphene and their use to obtain graphene concrete.

Thickness of the surface layer of graphite

The thickness of the surface layer of a solid R(I) is given by the formula:

$$R(I) = \alpha \cdot \frac{\upsilon}{S}[m]. \qquad (1)$$

In equation (1): the molar volume of the element $\upsilon = M/\rho$ (M is the molar mass, ρ is its density), $\alpha = 0.17\ 10^{-9}$ mol, $S = 1\ m^2$.

A schematic representation of equation (1) is shown in Fig. 1.

For graphite and graphene, the thickness of the surface layer R(I) is given in Table 1.

The elastic parameters of graphene and graphite are presented in Table 2. In Table 2, the value W_a represents the adhesion energy, and E is the Young's modulus of elasticity.

In Table 1, the number in brackets represents the number of monolayers – n = R(I)/a (a is the lattice constant). The number of graphite monolayers is 3, which is confirmed experimentally (Fig. 2).

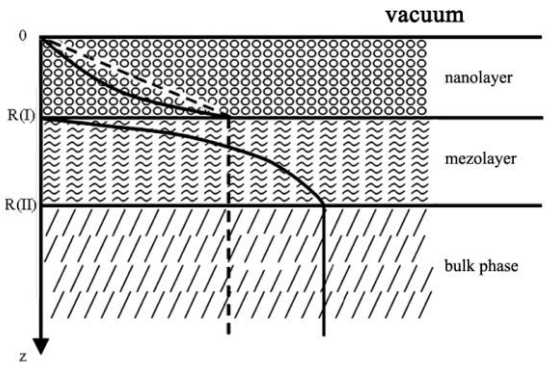

Figure 1 - Graphite diagram: nanolayer → mesolayer → bulk phase

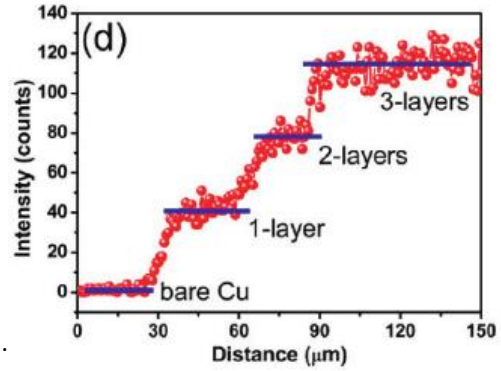

Figure 2 - Change in graphite parameters depending on the number of its monolayers [10].

We will calculate the estimate of the deformation energy associated with the reconstruction of the graphite surface using the formula:

$$E_d = \frac{1}{n} W_a \cdot R(I)^2. \qquad (2)$$

These data are shown in Table 3.

Table 1 - Surface layer thickness R(I) of graphite and graphene

Carbon	M, g/mol	ρ, g/sm^3	R(I)$_a$, nm	R(I)$_c$, nm	γ$_a$, mJ/m^2	γ$_c$, mJ/m^2
Graphite	12.0107	2.26	0.900 (3)	2.46 (3)	2195	130
Graphene	12.0107	2.26	0.246 (1)	0.14 (1)	2652	-

Table 2 - Elastic parameters of graphite and graphene

Carbon	W_{aa}, J/m^2	W_{ac}, J/m^2	σ_{isa}, GPa	σ_{isc}, GPa	E_a, GPa	E_c, GPa
Graphite	2.853	1.690	4.9	1.36	7.59	3.48
Graphene	3.448	-	118.4	-	1000	-

Table 3 - Deformation energy E_d of graphite and graphene

Carbon	E_{da}, eV	E_{dc}, eV
Graphite	2.27	1.42
Graphene	1.62	-

Figure 3 shows the corrugations on the graphene surface, which arise due to high internal stresses σis (Table 2), leading to significant deformation energy (Table 3).

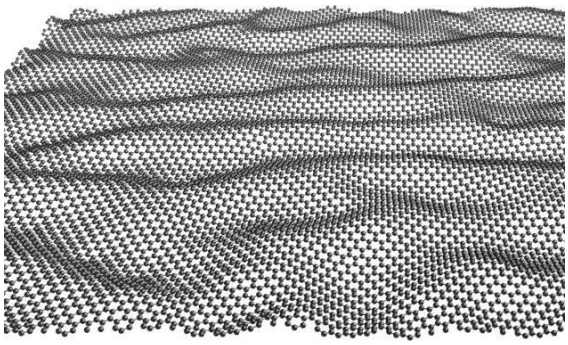

Figure 3 - Corrugated graphene

Figure 3 shows the occurrence of macrowaves on the graphene surface. We will represent a nanolayer with an area of S = 1 m^2 and a size of R(I) of graphite as a nonlinear capacitor - a varicond (due to the presence of size effects) on one of the plates of which large stresses σis develop, leading to significant deformation energy E_d (Table 3). This deformation energy first charges the capacitor, and then, under external influence (impact, friction, ultrasound, etc.), it is discharged (Fig. 4).

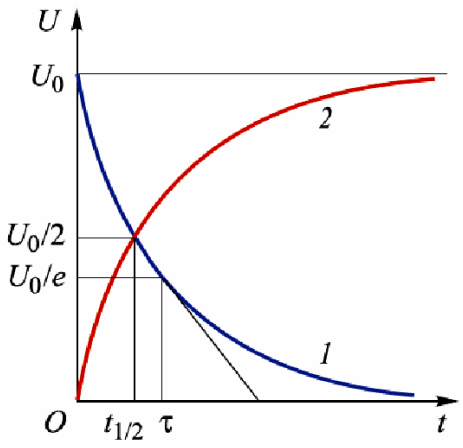

Figure 4 - Voltage change curves on the capacitor plates during its charging (1) and discharging (2)

The deformation energy E_d is spent on heat, acoustic emission (propagation of sound waves) (see below), exoemission (emission of slow electrons and ions) and luminescence.

Quantum structure of the surface layer of graphite

We will imagine the nanolayer in Fig. 1 as a potential well with infinitely high walls, then the energy levels $E_n(z)$ in it are equal to [11]:

$$Å_n(z) = \frac{\hbar^2\pi^2 n^2}{2m_e R(I)^2}, \qquad (3)$$

These levels are shown in Fig. 5a taking into account Table 1. The E_n level can be represented by Landau levels (Fig. 5b).

From equation (3) it follows that the energy levels E_n of the nanolayer are determined by one fundamental parameter – the crystal lattice constant **a** (this follows from n = R(I)/**a**):

$$Å_n(z) = \eta \cdot \frac{n^2}{à^2}, \qquad (4)$$

where η = const.

The lattice constant **a** changes in the R(I) layer due to the reconstruction of the graphite surface. This means that graphite monolayers can be represented as quantum planes with energy E_n. As soon as the parameter a stops changing, the spectrum of quantum states becomes a continuous spectrum, where the classical Drude–Lorentz laws are satisfied for graphite.

It follows from Fig. 5a that the energy level $E_n(\infty) = E_F$ is the Fermi energy level of graphite. In [12], the Fermi energy was calculated to be 1.5 eV for three-dimensional graphite and 2.0 eV for two-dimensional graphite. Since the surface layer of graphite is a two-dimensional medium, three quantum planes of graphite with $\mathbf{a_1}$, $\mathbf{a_2}$ and $\mathbf{a_3}$ should be considered. The first monolayer of graphite, graphene, determines unique physical and chemical properties [[13], [14]]. The motion of electrons in graphene is described by a two-component equation similar to the Dirac equation [13]. If we look for a solution to the Dirac equation in the form of a harmonic wave, we obtain the dispersion law for massless particles (Fig. 6) E = ± V_F k, and the solution itself has the form:

$$\tilde{N} = \frac{1}{\sqrt{2}} \cdot \begin{pmatrix} 1 \\ \pm e^{i\theta} \end{pmatrix} \cdot e^{ikr}, \theta = \mathrm{arctg}(k_y / k_x).$$

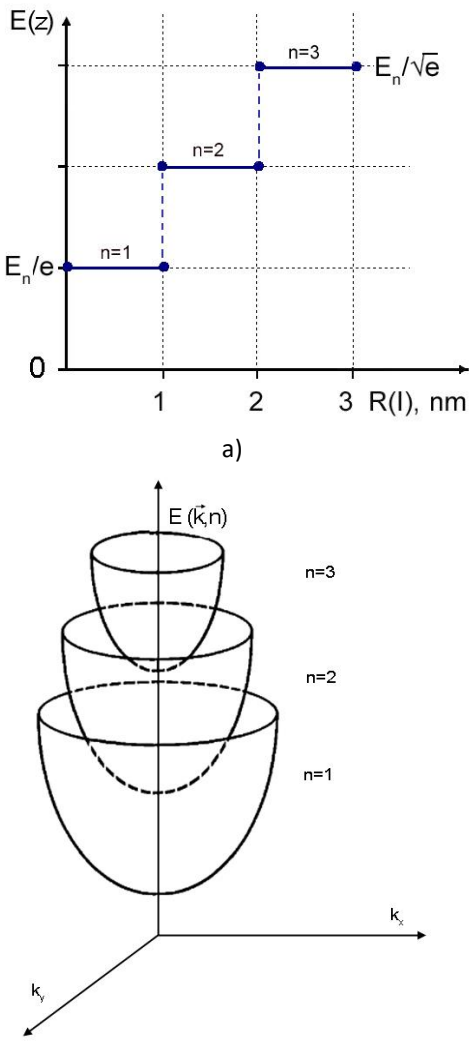

Figure 5 - Dependence of the energy level En in the nanolayer (a); quasi-discrete spectrum of electrons in the quantum well (b).

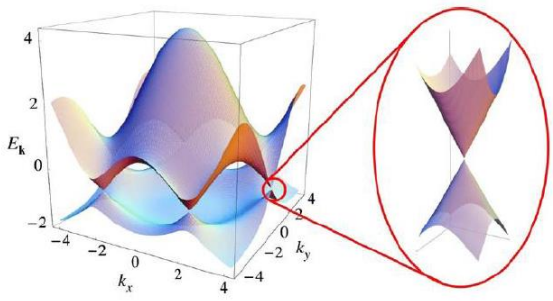

Figure 6 - Electronic structure of graphene [13].

The Fermi surface degenerates into the Dirac point (Fig. 6), and the Fermi energy is $E_F = 0$. Thus, graphene is a single-layer 2D Dirac material and is a quantum system at any temperature. The topological properties of graphene are due to the Dirac nature of the electron spectrum, which is similar to d-wave superconductors (cuprates, YBCO), which are also described by a massless Dirac Hamiltonian near the nodal points of the spectrum [15].

Bilayer graphene is different from monolayer graphene and graphite and exhibits improved physical, chemical, electronic and optical properties compared to graphene and bulk graphite materials [16]. Twisted bilayer graphene (tBLG) superlattice is formed when these layers are twisted at a small angle. The presence of disorder and interlayer interactions in tBLG improves several properties including optical and electrical properties. The studies of twisted bilayer graphene have been exciting and challenging so far, especially after the magic angle superconductivity was reported in tBLG [17]. Bilayer graphene can be considered as a “graphene + YBCO” system in the Landau–Zener model. We have shown that the superconducting transition temperature will be equal to:

$$\check{N}_{ń} = \frac{E_F}{k\ln(k\,\tau/2)} = \delta \cdot E_F, \qquad (5)$$

where δ = const, which is quite difficult to determine theoretically.

For us, the most important thing here is the dependence of the superconducting transition temperature on the Fermi energy E_F, which can be changed, for example, using magnetic or electric fields, or by changing the value of the magic angle. From Fig. 5a, taking into account the work [12], it follows that E_F for two-layer graphene is E_F=0.9 eV. In the work [18], for two-layer graphene, T_c = 1.7 K was obtained, which means that in (6) the value δ_1=1.9 K eV^{-1}.

Three-layer graphene differs from the latter two in mobility and conductivity [19]. A special feature of three-layer graphene is that after its magic-angle torsion, it develops superconductivity, which can withstand magnetic fields 2-3 times greater than the Pauli limit for spin-singlet pairing [20]. This case is similar to two-layer graphene, which can also be considered using the Landau–Zener Hamiltonian. From Fig. 5a, taking into account the work [12], it follows that the Fermi energy for three-layer graphene is E_F = 1.2 eV. In [21], it was obtained for three-layer graphene that T_c = 2.9 K, which means that in (6) the value δ_2 = 2.4 K eV^{-1}. Approximately, $\delta_1 = \delta_2 = 2$ = const is satisfied. The diagram of three-layer graphene is shown in Fig. 7.

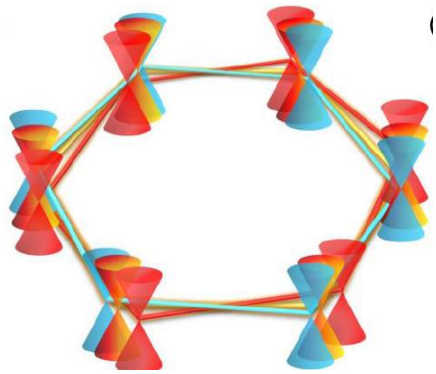

Figure 7 - Schematic Dirac cones of three graphene layers [22].

Acoustoemission of graphite and graphene

The essence of acoustoemission is the analysis of the parameters of extremely weak ultrasonic radiation accompanying any change in the structure of a solid, especially during its deformation (Fig. 8).

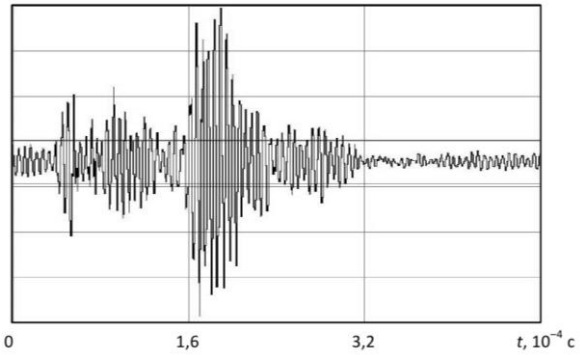

Figure 8 - Typical picture of the fine structure (oscillations) of acoustic emission signals recorded by a sensor on the surface of the body under study [23].

The total energy of the AE E_{AE} is equal to [23]

$$Ĺ_{ŕÝ} = \frac{\sigma_0^2 \cdot \lambda \cdot [R(I)]^2}{8\rho \cdot \upsilon^2}, \qquad (6)$$

where σ_0 is the maximum amplitude of elastic vibration stress; λ is the vibration wavelength; ρ is the density of the solid; υ is the speed of sound.

The maximum value of the wavelength λ propagating in a discrete chain of carbon along the z axis is equal to $R(I)_c$. The speed of sound in the surface layer of graphite is equal to υ = R(I)/τ, where τ is the relaxation time. For longitudinal modes, the relaxation time is τ_L = 0.2 10^{-12} s, for transverse modes – τ_T =2 10^{-12} s. For graphite, the speed of sound is shown in Table 4.

Table 4 - Speed of sound of longitudinal and transverse modes in graphite and graphene

Graphite	υ_L, m/s	υ_T, m/s
ρ = 2260, kg/m^3	4500	2380
ρ = 1986, kg/m^3 [24]	3505	1854
ρ = 1753, kg/m^3 [24]	2631	1591
Graphene	υ_L, м/с	υ_T, м/с
ρ = 0,77, mg/m^2 [[25], [26]]	19700	10700

In Table 4, lines 2 and 3 are taken from the work [24], where the values of the speed of sound in graphite were determined in samples of different densities. It is evident that the speed of sound increases with increasing crystal density.

On the contrary, the density of graphene is significantly lower than that of graphite [25], but the speed of sound in it is almost 5 times greater than that of graphite [26].

In equation (6), we take $\sigma_0 = \sigma_{is}$, then for the E_{AE} we obtain the values (Table 5).

Table 5 - AE energy

Carbon	E_{AEa}, eV	E_{AEc}, eV
Graphite	2.98	1.86
Graphene	2.13	-

Comparing Table 3 with Table 3, it is evident that the deformation energy E_d of graphite and graphene, arising due to the reconstruction of their surface, coincides within the experimental error with the acoustic emission energy E_{AE}, i.e. $E_d \approx E_{AE}$.

Thus, it can be considered proven that in natural graphite (as in all solids), acoustic emission arises due to the reconstruction of its surface, leading to the emergence of a surface layer R(I) and deformation energy E_d.

Let us transform formula (6). As a result, we obtain:

$$Ĺ_{ŕÝ} = \frac{4{,}6 \cdot T_m \cdot E \cdot R(I)}{M} \cdot (eV), \qquad (7)$$

where T_m is the melting point of the solid (K); E is the Young's modulus (GPa); M is the mass of the crystal (kg).

From formula (7) it follows that the value of the E_{AE} is proportional to the temperature, and this allows graphene to be used as a thermophone - a device in which thermoacoustics forces heat to be converted into sound [27]. Such a graphene

thermophone differs from speakers and piezoelectric transducers by the complete absence of mechanical moving elements (Fig. 9).

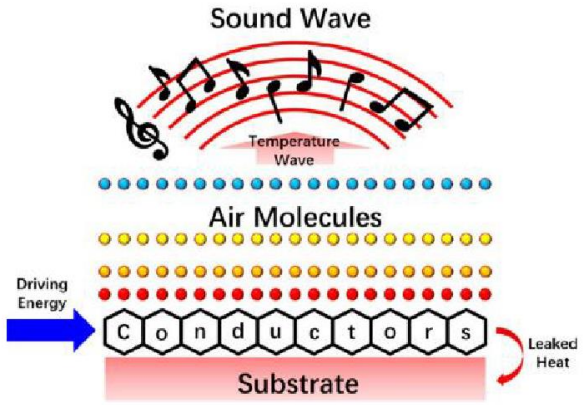

Figure 9 - Operating principle of the hydroacoustic transducer [27]

The first thermoacoustics model was proposed in 1917 and the last one in 2018 (see review in [27]), but only qualitative estimates were obtained.

Our model, represented by equation (7), contains only experimentally determined parameters and their accuracy is quite acceptable.

The value of the acoustic emission energy in formula (7) is proportional to R(I).

Cracks determine the performance of all existing structures and are studied by the acoustic emission method (see bibliography in [[28], [29]].

In 2019, the International Organization for Standardization (ISO) developed three new standards:

ISO 16836. Non-destructive testing. Acoustic emission testing. Method for measuring AE signals in concrete;

ISO 16837. Non-destructive testing. Acoustic emission testing. Method for qualifying damage assessment in reinforced concrete beams;

ISO 16838. Non-destructive testing. Acoustic emission testing. Method for classifying active cracks in concrete structures.

We have shown that the evolution of nanocracks occurs according to the law:

$$L_C = 10^2 L_{\mu m} = 10^4 L_{nm} = 0{,}17 \cdot 10^{-5} \frac{M}{\rho} \quad (8)$$

where L_{nm}, $L_{\mu m}$, L_C are the lengths of nanocracks, mesocracks and the critical length of cracks before the destruction of a solid.

Equation (8) shows: the number of cracks in concrete in the region of nanostructure I is 10^5, in mesoscopic II it is 10^7 and in the pre-destruction region III it is about 10^9.

Adding graphene to cement mortar significantly strengthens (by 4-5 times) standard concrete and reduces the number of nanocracks.

Conclusion

The energy of deformation is created during the reconstruction of graphite and all other solids, and even liquids, when they are finite and in contact with either a vacuum or the external environment. The energy of deformation is spent on heat, acoustic emission (propagation of sound waves), exoemission (emission of slow electrons and ions) and luminescence. This is the mechanism of graphite acoustic emission. In this case, the surface layer of graphite and graphene, which is obtained by splitting graphite, are responsible for acoustic emission.

Conflict of interest. On behalf of all the authors, the correspondent author declares that there is no conflict of interest.

CRediT author statement: **K.Zhangozin** Methodology. Data curation; **V.Yurov:** Calculations of parameters. Drawing up figures and tables; **D.Kargin :** Reviewing and editing.

Acknowledgements. This scientific article was published as part of the grant funding for 2024-2026 IRN No. AP32488258 "Development of an innovative technology for obtaining graphene by intercalating graphite with microcluster water and modifying HTSC ceramics with graphene" (the study is funded by the Science Committee of the Ministry of Science and Higher Education of the Republic of Kazakhstan).

Cite this article as: Zhangozin KN, Yurov VM, Kargin DB. Acoustoemission of Graphite and Graphene. Kompleksnoe Ispolzovanie Mineralnogo Syra = Complex Use of Mineral Resources. 2026; 338(3):92-100. https://doi.org/10.31643/2026/6445.32

Графит пен графеннің акустикалық эмиссиясы

[1*] Жангозин К.Н., [2] Юров В.М., [3] Каргин Д.Б.

[1] ТСК-Восток ЖШС, Астана, Қазақстан
[2] ТСК-Восток ЖШС, Қарағанды, Қазақстан
[3]Л.Н.Гумилев атындағы Еуразия ұлттық университеті, Астана, Қазақстан

Мақала келді: *26 ақпан 2025*
Сараптамадан өтті: *15 сәуір 2025*
Қабылданды: *2 мамыр 2025*

ТҮЙІНДЕМЕ

Мақалады табиғи графит пен графеннің акустикалық эмиссия механизмінің үлгісі ұсынылады. Графиттің беткі қабатының R (I) қалыңдығы параллель жазықтықта 0,9 нм-ден перпендикуляр жазықтықта 2,46 нм-ге дейін өзгереді және үш графен моноқабаттарын қамтиды. Еркін графеннің бетіндегі гофрлар айтарлықтай деформация энергиясына әкелетін жоғары ішкі кернеулерден туындайды. Графит пен графеннің бетін қалпына келтіруге байланысты деформация энергиясын бағалау ұсынылады. Біз графитті наноқабатты шексіз биік қабырғалары бар потенциалды ұңғыма ретінде елестетеміз, содан кейін наноқабаттың энергетикалық деңгейлері бір іргелі параметрмен – кристалдың кристалдық тор тұрақтысымен анықталады. Кристалдық тор константасы R(I) қабатында өлшемдік әсерлерге байланысты өзгереді. А параметрі өзгеруін тоқтатқаннан кейін кванттық күйлер спектрі үздіксіз спектрге айналады, мұнда графит үшін классикалық Друд-Лоренц заңдары орындалады. Графиттің беткі қабаты екі өлшемді кванттық орта болғандықтан, графиттің a_1, a_2, a_3 және болатын үш кванттық жазықтығы қарастырылуы керек. Мақалада бір, екі және үш қабатты графен қарастырылады. Графеннің Ферми беті Дирак нүктесіне айналады, ал Ферми энергиясы нөлге тең. Екі қабатты графен үшін Ферми энергиясы E_F = 0,9 эВ, ал үш қабатты графен үшін E_F = 1,2 эВ. Атап айтқанда, осы кванттық деңгейлердің үшеуі де графит пен графеннің акустикалық эмиссиясына қатысады. Мақалада табиғи графитте (барлық қатты денелердегі сияқты) акустикалық эмиссия оның бетінің қайта құрылуына байланысты пайда болып, беттік қабаттың R(I) түзілуіне әкелетіні және деформация энергиясы Ed болатыны дәлелденген деп санауға болады. Мақалада тек эксперименталды түрде анықталған параметрлерді қамтитын термоакустика моделі ұсынылған және олардың дәлдігі әбден қолайлы.

Түйін сөздер: акустикалық эмиссия, графит, графен, наноқабат, Ферми беті, кристалл.

Авторлар туралы мәліметтер:

Жангозин Канат Нәкешұлы — *ТСК-Восток ЖШС директоры, жетекші ғылыми қызметкер, физика-математика ғылымдарының кандидаты, доцент, Сарыарқа ауданы, Республика даңғылы, 3/2 корпус, 40-пәтер, Астана, Қазақстан. E-mail: 4kzh@mail.ru; ORCID ID: https://orcid.org/0000-0003-1234-0486*

Юров Виктор Михайлович — *ТСК-Восток ЖШС жетекші ғылыми қызметкері, физика-математика ғылымдарының кандидаты, доцент, Гоголь көшесі 51 пәтер 55, Қарағанды, Қазақстан. E-mail: exciton@list.ru; ORCID ID: https://orcid.org/0000-0002-7918-9656*

Қаргин Жұмат Бейсенбекұлы — *Л.Н. Гумилев атындағы Еуразия ұлттық университетінің физика-математика ғылымдарының кандидаты, доцент, ғылыми қызметкер, Сәтбаев көшесі, 2-ғимарат, Астана, Қазақстан. E-mail: kargin_db@enu.kz; ORCID ID: https://orcid.org/0000-0002-1027-6428*

Акустоэмиссия графита и графена

[1*]Жангозин К.Н., [2]Юров В.М., [3]Каргин Д.Б.

[1]ТОО ТСК-Восток, Астана, Казахстан
[2]ТОО ТСК-Восток, Караганда, Казахстан
[3]НАО Евразийский национальный университет имени Л.Н. Гумилева, Астана, Казахстан

Поступила: *26 февраля 2025*
Рецензирование: *15 апреля 2025*
Принята в печать: *2 мая 2025*

АННОТАЦИЯ

В настоящей статье предлагается модель механизма акустоэмиссии натурального графита и графена. Толщина поверхностного слоя R(I) графита изменяется от 0,9 нм в параллельной до 2,46 нм в перпендикулярной плоскости и содержит три графеновых монослоя. Гофры на поверхности свободного графена возникают за счет высоких внутренних напряжений, приводящих к значительной энергии деформации. Предложена оценка энергии деформации, связанной с реконструкцией поверхности графита и графена. Нанослой графита представим как потенциальную яму с бесконечно высокими стенками, тогда уровни энергии нанослоя определяются одним фундаментальным параметром – постоянной кристаллической решетки кристалла. Постоянная кристаллической решетки а изменяется в слое R(I) из-за размерных эффектов. Как только параметр а перестает

изменяться, спектр квантовых состояний переходит в непрерывный спектр, где для графита выполняются классические законы Друде–Лоренца. Поскольку поверхностный слой графита представляет собой двумерную квантовую среду, то следует рассматривать три квантовые плоскости графита с a_1, a_2 и a_3. В статье рассмотрен одно-двух-трехслойный графен. Поверхность Ферми у графена вырождается в точку Дирака, а энергия Ферми равна нулю. Для двухслойного графена энергия Ферми равна E_F = 0,9 эВ, а для трехслойного графена - E_F = 1,2 эВ. Именно, все эти три квантовых уровня участвуют в акустической эмиссии графита и графена. В статье можно считать доказанным, что в природном графите (как и всех твердых телах) акустическая эмиссия возникает из-за реконструкции его поверхности, приводящая к возникновению поверхностного слоя R(I) и энергии деформации E_d. В статье предложена модель термоакустики, которая содержит только экспериментально определяемые параметры и точность их довольно приемлема.

Ключевые слова: акустоэмиссия, графит, графен, нанослой, поверхность Ферми, кристалл.

Сведения об авторах:

Жангозин Канат Накошевич *Директор ТОО ТСК-Восток, ведущий научный сотрудник кандидат физико-математических наук, доцент, район Сарыарка, проспект Республика, дом 3/2, квартира 40, Астана, Казахстан. E-mail: 4kzh@mail.ru; ORCID ID: https://orcid.org/0000-0003-1234-0486*

Юров Виктор Михайлович *Ведущий научный сотрудник ТОО ТСК-Восток, кандидат физико-математических наук, доцент, улица Гоголя 51, квартира 55, Караганда, Казахстан. E-mail: exciton@list.ru; ORCID ID: https://orcid.org/0000-0002-7918-9656*

Каргин Джумат Бейсенбекович *Кандидат физико-математических наук, доцент, исследователь Евразийского национального университета им. Л.Н. Гумилева, улица Сатпаева, дом 2, Астана, Казахстан. E-mail: kargin_db@enu.kz; ORCID ID: https://orcid.org/0000-0002-1027-6428*

References

[1] Savvatimskii AI. Plavleniye grafita i zhidkogo ugleroda [Melting of graphite and liquid carbon]. Uspekhi Fizicheskikh Nauk [Advances in Physical Sciences]. 2003; 173(12):1371-1379. (in Russ.).

[2] Jmurikov EI, Bubnenkov IA, Dremov VV, Samarin SI, Pokrovskii AS, Harkov DV. Grafit v nauke i yadernoi tehnike [Graphite in science and nuclear engineering]. Novosibirsk. 2013, 193. (in Russ.).

[3] Panyukov SV, Subbotin AV, Arzhakov MV. Dimensional changes in bulk graphite caused by irradiation: Theory. Zhurnal Yadernykh Materilov. 2013; 439(1-3):72-83. https://doi.org/10.1016/j.jnucmat.2013.03.070

[4] Kroto HW, Heath JR, O'Brien SC, Curl RF, Smalley RE. C60: Buckminsterfullerene. Nature. 1985; 318:162-163. https://doi.org/10.1038/318162a0

[5] Iijima S. Helical microtubebules of graphitic carbon. Nature. 1991; 354(6348):56-58. https://doi.org/10.1038/354056a0

[6] Novoselov KS, Geim AK, Morozov SV, Jiang D, Zhang I, Dubonos SV, Grigorieva IV, Firsov AA. Electric field effect in atomically thin carbon films. Science. 2004; 306(5696):666-669. https://doi.org/10.1126/science.1102896

[7] Wu Y, Qiao P, Chong T, Shen Z. Carbon nanowalls grown by microwave plasma-enhanced chemical vapor deposition. Advanced Materials. 2002; 14(1):64-67.

[8] Panin VE, Sergeev VP, Panin AV. Nanostrukturirovanie poverhnostnih sloev konstrukcionnih materialov i nanesenie nanostrukturnih pokritii [Nanostructuring of surface layers of structural materials and application of nanostructured coatings]. Tomsk. Izd vo TPU. 2010, 254. (in Russ.).

[9] Muraveva OV, Blinova AV, Denisov LA, Bogdan OP. Osobennosti rasprostraneniya akusticheskih normalnih voln v tonkih poristih listah termorasshirennogo grafita [Features of Propagation of Acoustic Normal Waves in Ton-Porous Sheets of Thermally Expanded Graphite]. Pribori i metodi izmerenii. 2024; 15(3):213-230. (in Russ.).

[10] Abidi IH, Weng L-T, Wong KPJ, Tyagi A, Gan L, Ding Y, et al. A New Approach to Revealing Individual Atomic Layers of 2D Materials and Their Heterostructures. Chemistry of Materials. 2018; 30(5):1718-1728. https://doi.org/10.1021/acs.chemmater.7b05371

[11] Landau LD, Lifshic EM. Kurs teoreticheskoi fiziki. Kvantovaya mehanika _nerelyativistskaya teoriya [Course of Theoretical Physics. Quantum Mechanics (Nonrelativistic Theory)]. M.Fizmatlit. 2004; III:800. (in Russ.).

[12] Moliver SS. Oje_spektroskopicheskoe proyavlenie korrelyacii elektronov poverhnosti Fermi grafita [Auger Spectroscopic Manifestation of Electron Patterns on the Fermi Surface of Graphite]. Fizika tverdogo tela. 2004; 46(9):1537-1543. (in Russ.).

[13] Novoselov KS. Grafen_ materiali Flatlandii [Graphene: Materials of Flatland]. Uspehi fizicheskih nauk. 2011; 181(12):1299-1311. (in Russ.). https://doi.org/10.3367/UFNr.0181.201112f.1299

[14] Zhang T. Graphene. From Theory to Applications. Springer. 2022, 142.

[15] Ostrovskii PM. Elektronnie svoistva neuporyadochennogo grafena [Electronic Properties of Disordered Graphene]. Dissertaciya doktora fiz._mat. nauk_ Chernogolovka. 2019, 227. (in Russ.).

[16] Rozhkov AV, Sboychakov AO, Rakhmanov AL, Nori F. Electronic Properties of Graphene-Based Bilayer Systems. Physics Reports. 2016; 648:1-104. http://dx.doi.org/10.1016/j.physrep.2016.07.003

[17] Nimbalkar A, Kim H. Potential and Challenges of Twisted Bilayer Graphene: A Review. Nano-Micro Lett. 2020; 12(126):125-145. https://doi.org/10.1007/s40820-020-00464-8

[18] Sboychakov AO, Rozhkov AV, Rakhmanov AL. Magic radius of the quantum dot of bilayer AA graphene. Modern Electrodynamics. 2022; 1(1):6-13. https://doi.org/10.1103/PhysRevB.105.235415

[19] Codecido E, Wang QY, Koester R, Che S, Tian HD. Correlated insulating and superconducting states in twisted bilayer graphene below the magic one. Sci. Adv. 2019; 5(9):eaaw9770. https://doi.org/10.1126/sciadv.aaw9770

[20] Lu X, Stepanov P, Yang W, Xie M, Aamir MA, Das I, Urgell C, Watanabe K, Taniguchi T, Zhang G, Bachtold A, MacDonald AH, Efetov DK. Superconductors, orbital magnets, and correlated states in bilayer magic-angle graphene. Nature. 2019; 574(7780):653-657. https://doi.org/10.1038/s41586-019-1695-0

[21] Craciun MF, Russo S, Yamamoto M, Oostinga JB, Morpurgo AF, and Tarucha S. Trilayer graphene is a semimetal with a gate-tunable band overlap. Nature Nanotechnology. 2009; 4:383-388. https://doi.org/10.1103/PhysRevX.2.011004

[22] Devakul T, Ledwith PJ, Xia L-Q, Uri A, de la Barrera S, Jarillo-Herrero P, and Fu L. Magic-angle helical trilayer graphene. Science Advances. 2023; 9(36):eadi6063. https://doi.org/10.1126/sciadv.adi6063

[23] Builo SI. Fiziko_mehanicheskie_ statisticheskie i himicheskie aspekti akustiko_emissionnoi diagnostiki [Physicomechanical, statistical and chemical aspects of acoustic emission diagnostics]. Rostov_na_Donu; Taganrog_ Izdatelstvo Yujnogo federalnogo universiteta. 2017, 184. (in Russ.).

[24] Kuleev II, Kuleev IG, Baharev SM, Inyushkin AV. Vremena relaksacii i dlini svobodnogo probega fononov v rejime granichnogo rasseyaniya dlya monokristallov kremniya [Relaxation times and mean free paths of phonons in the boundary scattering regime for silicon single crystals]. Fizika tverdogo tela. 2013; 55(1):24-35. (in Russ.).

[25] Kokshaiskii AI, Shirgina NV, Korobov AI, Prohorov VM. Issledovanie akustouprugogo effekta v grafite [Study of the acoustoelastic effect in graphite]. Trudi shkoli_seminara Volni-2017. Akustika i akustooptika. 2017, 44-46. (in Russ.).

[26] Baimova YuA, Dmitriev SV, Savin AV, Kivshar YuS. Skorosti zvuka i plotnosti fononnih sostoyanii v odnorodno deformirovannom ploskom liste grafena [Sound velocities and phonon state densities in a uniformly deformed flat graphene sheet]. Fizika tverdogo tela. 2012; 54(4):813-820. (in Russ.).

[27] Boiko EV. Termoakustika grafenovih pokritii i vliyanie grafenovogo pokritiya na teplootdachu [Thermoacoustics of graphene coatings and the effect of graphene coating on heat transfer]. Dissertaciya kandidata fiz._mat. Nauk. Novosibirsk. 2024, 101. (in Russ.).

[28] Chernov DV. Razrabotka metodov diagnostiki ustalostnih treschin s pomoschyu akusticheskoi emissii [Development of methods for diagnosing fatigue cracks using acoustic emission]. Dissertaciya kandidata tehnicheskih nauk. Moskva. 2018, 148.

[29] Grigorev EV. Obosnovanie metoda kontrolya vliyaniya uprochnyayuschih obrabotok svarnih soedinenii na osnove rezultatov registracii signalov akusticheskoi emissii [Justification of the method for monitoring the influence of hardening treatments of welded joints based on the results of recording acoustic emission signals]. Dissertaciya kandidata tehnicheskih nauk. Sankt–Peterburg. 2024, 131. (in Russ.).